International Journal of Pharmaceutics 372 (2009) 169–176

Contents lists available at ScienceDirect

International Journal of Pharmaceutics

journal homepage: www.elsevier.com/locate/ijpharm

Pharmaceutical Nanotechnology

Superparamagnetic iron oxide nanoparticles-loaded chitosan-linoleic acid nanoparticles as an effective hepatocyte-targeted gene delivery system

Su-Jin Cheong[a,b,c,1], Chang-Moon Lee[a,b,c,1], Se-Lim Kim[a,b,c], Hwan-Jeong Jeong[a,b,c,*], Eun-Mi Kim[a,b,c], Eun-Hye Park[a,b,c], Dong Wook Kim[a,b,c], Seok Tae Lim[a,b,c], Myung-Hee Sohn[a,b,c]

[a] Department of Nuclear Medicine, Chonbuk National University Medical School and Hospital, Jeonju 561-756, Republic of Korea
[b] Research Institute of Clinical Medicine, Chonbuk National University Medical School and Hospital, Jeonju 561-756, Republic of Korea
[c] Institute for Medical Science, Chonbuk National University Medical School and Hospital, Jeonju 561-756, Republic of Korea

ARTICLE INFO

Article history:
Received 16 September 2008
Received in revised form 8 January 2009
Accepted 10 January 2009
Available online 20 January 2009

Keywords:
Gene delivery
Superparamagnetic iron oxide nanoparticles
Chitosan
Linoleic acid
Hepatocyte
Molecular imaging

ABSTRACT

The goal of this study was to develop a gene delivery imaging system that targets hepatocytes to help diagnose and treat various liver diseases. To this end, we prepared superparamagnetic iron oxide nanoparticles (SPIO)-loaded with water-soluble chitosan (WSC)-linoleic acid (LA) nanoparticles (SCLNs) that formed gene complexes capable of localizing specifically to hepatocytes. We confirmed that ^{99m}Tc-labeled SCLNs delivered into mice via intravenous injection accumulated mainly in the liver using nuclear and magnetic resonance imaging. SCLN/enhanced green fluorescence protein (pEGFP) complexes were also successfully formed and were characterized with a gel retardation assay. SCLN/pEGFP complexes were transfected into primary hepatocytes, where GFP expression was observed in the cytoplasm. In addition, the injection of the gene complexes into mice resulted in significantly increased expression of GFP in hepatocytes *in vivo*. Furthermore, gene silencing was effectively achieved by administration of gene complexes loaded with specific siRNAs. In conclusion, our results indicate that the SCLNs have the potential to be useful for hepatocyte-targeted imaging and effective gene delivery into hepatocytes.

1. Introduction

Gene therapy is one of several new therapeutic approaches for the treatment of human incurable diseases and genetic disorders. Successful gene therapy requires the development of innovative gene delivery vectors. Viral vectors have been extensively used to deliver genetic information to human cells (Walther and Stein, 2000). However, the clinical applications of viral vectors are limited due to safety considerations. In contrast, non-viral vectors are potentially useful for effective gene transfer due to their decreased pathogenicity, low immune reactivity, and non-toxicity. A number of non-viral vectors, such as cationic polymers, lipids, and proteins have been reported to accomplish efficient gene delivery and transfection (Davis, 2002). Of the reported non-viral vectors, chitosan and chitosan derivatives have been proposed as a promising cationic polymer for suitable gene delivery (Erbacher et al., 1998). Chitosan has many advantages, such as low toxicity, low immunogenicity, biodegradation, high DNA binding efficiency and transfection efficiency (Richardson et al., 1999; Borchard, 2001; Mansouri et al., 2004; Gao et al., 2005). Moreover, through the complex formation, chitosan can protect the DNA from degradation by nucleases. Of these advantages, the alternative property of chitosan has free amino and hydroxyl groups, and thus can be easily conjugated with target ligands. Recently, we reported the usefulness of chitosan derivatives in hepatocyte imaging (Kim et al., 2006).

Hepatocytes are considered as a target for gene therapy because there are many fetal metabolic diseases that result from the presence of defective or deficient hepatocyte-derived gene products as well as infestation of many different types of viruses (Ponder, 1996). To overcome these diseases, the development of gene delivery systems that can deliver therapeutic genes selectively to hepatocytes *in vivo* is invaluable. Two approaches to target hepatocytes have been intensively explored (Nishikawa et al., 1998; Wu et al., 2002). The first targeting method involves the asialoglycoprotein receptor (ASGP-R) recognition pathway, while the other involves a lipid metabolism pathway (Wu et al., 2002; Adrian et al., 2007).

Linoleic acid (LA) is one of essential polyunsaturated fatty acids. When it is administrated into the body, LA accumulates into hepatocytes and plays a central role in the liver (Thomas et al., 1988). Thus, LA is often used as a trigger to mediate uptake into hepatocytes (Pandey et al., 2008). Interestingly, LA has been also used as a

* Corresponding author at: Department of Nuclear Medicine, Chonbuk National University Medical School, 634-18, Geumam-2 dong, Duckjin-gu, Jeonju City 561-712, Republic of Korea. Tel.: +82 63 250 1674; fax: +82 63 250 1676.
E-mail address: jayjeong@chonbuk.ac.kr (H.-J. Jeong).
[1] These authors contributed equally to this study.

0378-5173/$ – see front matter © 2009 Elsevier B.V. All rights reserved.
doi:10.1016/j.ijpharm.2009.01.009

hydrophobic moiety for the formation of self-assembled nanoparticles (Liu et al., 2005). For example, when LA is conjugated to water-soluble chitosan (WSC), self-assembled nanoparticles can be formed spontaneously.

In this study, LA was used as a hydrophobic segment to self-assemble nanoparticles and a trigger ligand to target hepatocytes. We synthesized WSC-LA conjugates for a gene delivery vector, and iron oxide nanoparticles (SPIONs) were loaded into the core of the nanoparticles formed by WSC-LA conjugates. SPIONs enhance the low innate contrast of biological molecules in magnetic resonance imaging (MRI) (Reimer et al., 2000; Bulte and Kraitchman, 2004). In particular, an imaging probe including SPION is useful for understanding the pharmacokinetics and pharmacodynamics of therapeutic compounds (Weissleder and Mahmood, 2001). In this study, we investigated that the SPION-loaded WSC-LA nanoparticles (SCLNs) are an effective gene delivery imaging system to target hepatocytes.

2. Materials and methods

2.1. Materials

Water-soluble chitosan (WSC, molecular weight: 10 kDa, deacetylation: 97%) was purchased from Kittolife Co. (Seoul, Korea). $Fe(acac)_3$ (iron (III) acetylacetonate), oleic acid, oleylamine, 1,2-hexadecanediol, phenyl ether, potassium ferrocyanide (II) trihydrate, linoleic acid (LA), *N*-hydroxysuccinimide (NHS), 1-ethyl-3-(3-(dimethylamino)-propyl) carbodiimide (EDC), and paraformaldehyde were purchased from Sigma–Aldrich Chemical Co. (St. Louis, MO). An enhanced green fluorescent protein (pEGFP) expression vector was purchased from Invitrogen Co. (Carlsbad, CA). Vector-specific siRNA was purchased from Bioneer Co. (Daejon, Korea). Animal experiments were conducted according to protocols approved by the Institutional Animal Care and Use Committee of our institution. ^{99m}Tc pertechnetate was eluted from a technetium generator produced by Samyoung Unitech (Seoul, Korea). All other chemicals were of analytical grade and were used directly without further purification.

2.2. Preparation and characterization of SCLNs

The synthesis of core SPIONs was performed as described previously with slight modifications (Sun et al., 2004). Briefly, SPIONs, 12 nm in size, were synthesized from 4 nm nanocrystals using a seed and growth method. WSC-LA conjugates were prepared by a 1-ethyl-3-(3-(dimethylamino)-propyl) carbodiimide (EDC)-mediated reaction (Jun et al., 2005). WSC (100 mg) was dissolved in the mixture solution of distilled water (10 ml) and methanol (8 ml). LA was then added to the WSC solution at a ratio of 0.5 mol/mol glucosamine residue to WSC. Equal mole ratios of EDC and LA were then dissolved in 2 ml of methanol and added dropwise to the WSC-LA solution under stirring at room temperature. After 24 h, the WSC-LA conjugates were separated and purified by dialysis against a mixture of methanol and distilled water, and the final solution was lyophilized. Conjugation was confirmed by ^{1}H NMR analysis. To load SPIONs into the WSC-LA nanoparticles, the WSC-LA (10 mg/ml) solution in PBS buffer (0.1 M, pH 7.4) was sonicated using a probe type sonifier (VCX 500, SONICS & MATERIALS Inc., CT, USA) at 25 W for 5 min at 4 °C. The SPION solution (0.1 mg/0.5 ml) in chloroform was then added to the WSC-LA solution and the mixture was sonicated for an additional 20 min at 4 °C. SCLNs were observed using an H-7650 electron microscope (Hitachi Ltd., Tokyo, Japan). The size distribution of SCLNs was determined by dynamic light scattering (DLS) using a Microtrac UPA-150 particle size analyzer (Microtrac Inc., Jeonju KBSI, Korea). Thermogravimetric analysis (TGA) was performed using a METTLER TOLEDO instrument (SDTA 851E, Greifensee, Switzerland).

2.3. Formation of SCLN/DNA complexes

A plasmid vector containing the enhanced green fluorescence protein (pEGFP) was transformed into *Escherichia coli* (DH5α) and purified using a Plasmid Mini Kit (Qiagen, Valencia, CA). SCLN/DNA complexes were prepared as described previously (Sagara and Kim, 2002). Briefly, pEGFP (0.5 μg) was added to the desired amount of the SCLNs solution, and the resulting mixture was incubated at room temperature for 30 min. To confirm the formation of complexes, we used 1% Tris-acetate (TAE) agarose gel electrophoresis analysis. Each sample containing a loading dye (2 μl) was loaded into its respective well and electrophoresed with a TAE running buffer at 100 V for 40 min. Visualization of DNA bands was carried out using a UV transilluminator (LAS-3000, Fuji Film, Japan) at 254 nm. In addition, to investigate the effectiveness of siRNA-mediated gene silencing, siRNA (0.3 μg) was simultaneously added into the SCLNs solution with the pEGFP solution. The size distribution of the SCLN/DNA complexes was determined using an ELS-8000 (Photal Otsuka Electronics Co., Japan).

2.4. Primary hepatocyte isolation and culture

Primary hepatocytes were isolated from a BALB/c mouse (female, 5–7 weeks old, Orient Co., Korea) using the collagenase perfusion method of Seglen (1976). After perfusion of the liver with Hanks' balanced salt solution (HBSS), the liver was digested with collagenase. Hepatocytes were purified from the dissected liver using a 45% Percoll solution and density-gradient centrifugation at 50 × *g* for 10 min at 4 °C. Cell viability was measured using a trypan blue dye exclusion assay, which indicated that more than 90% of the isolated cells were viable. Hepatocytes were cultured with serum-free William's medium E (WE) containing penicillin (50 μg/ml), streptomycin (50 μg/ml), and HEPES (18 mM).

2.5. Radiolabeling with ^{99m}Tc and cellular uptake of SCLNs

SCLNs were radiolabeled with ^{99m}Tc to allow *in vitro* monitoring of hepatocyte-targeted cellular uptake. Radiolabeling was carried out with a stannous chloride solution in 0.04N hydrochloric acid. ^{99m}Tc sodium pertechnetate eluate (9.25 MBq) in saline was added into a vial containing a mixture of $SnCl_2{\cdot}2H_2O$ and SCLNs. After a 30 min incubation period at room temperature, the labeling efficiency was evaluated by instant thin layer chromatography (ITLC) using acetone as the mobile phase. The paper strip was analyzed with a TLC scanner (AR-2000, Bioscan, Washington DC, USA).

Hepatocytes (1×10^6 cells) were incubated in serum-free culture media for 24 h, followed by incubation with various concentrations of ^{99m}Tc-labeled SCLNs (0.25, 1.25, and 2.5 μg/100 μl) for 1 h. For the competition study, non-radiolabeled SCLNs at 50 times the maximum concentration of ^{99m}Tc-labeled SCLNs was added simultaneously to the cells with the radiolabeled SCLNs. After washing the cells three times with HBSS, the cells were harvested and radioactivity of the cells was measured using a gamma counter (Cobra II PACKARD, USA).

2.6. Nuclear and MR imaging of SCLNs

Mice (BALB/C, female, 6 weeks old) were anesthetized by intraperitoneal injection of 0.05 ml of a ketamine/xylazine mixture (1:3 volume ratio), and ^{99m}Tc-labeled SCLNs (8.0 MBq) were injected into the tail vein. Static images were obtained using a

Table 1
Mean diameter and zeta potential of various complexes.

Complexes	SCLNs (μg)	pEGFP (μg)	siRNA (μg)	Mean diameter (nm)	Zeta potential (mV)
SCLNs/pEGFP	132	3	–	95.3 ± 10.5	49.8 ± 2.1
SCLN/pEGFP/siRNA	132	3	1.8	114.7 ± 37.9	49.8 ± 0.7

gamma camera (Vertex, ADAC, Milpitas, CA, USA) equipped with a low energy, parallel-hole collimator (40% window, 140 keV photopeak). The images were acquired at 30 min and 1 h after injection. MR imaging was performed using a 1.5 T clinical MR scanner with an animal coil (4.3 cm Quadrature volume coil, Nova Medical System, Wilmington, DE). After anesthetizing mice with 1.5% isoflurane in a 1:2 mixture of O_2/N_2, SCLNs (13 mg Fe/kg body) were injected intravenously through the tail vein. Fast spin echo T_2-weigthed images of the liver were obtained at 30 min, 1, and 2 h using the following parameters: TR = 4200 ms, TE = 102 ms, flip angle of 90°, echo train length of 10, 5 cm field of view, 2 mm section thickness, 0.2 mm intersection gap, and 256 × 160 matrix. One radiologist performed quantitative analysis of the MR images. The signal intensity (SI) of regions of interest (ROIs) in the liver were measured and compared with the back muscle adjacent to the liver. Relative signal enhancement was calculated by SI values before (SI pre) and after (SI post) injection of SCLNs according to the following formula: [(SI post − SI pre)/SI pre].

2.7. In vitro transfection into primary hepatocytes

For confocal microscopy, collagen-coated cover glasses (Iwaki, Tokyo, Japan) were placed in the wells of 24-well plates. Primary hepatocytes were seeded on the cover glasses at a density of 1×10^4 cells/well, and were incubated in serum-free culture medium for 24 h. SCLN/pEGFP, SCLN/pEGFP/siRNA, and SCLN/siRNA complexes were prepared as described for the gel retardation assay. Briefly, the complexes were diluted with serum-free media such that the ratio of complex/media was 1% (w/v, standard amount: DNA). The cells were then treated with pEGFP only, SCLN/pEGFP, SCLN/pEGFP/siRNA, or SCLN/siRNA complexes. Expression of the gene complexes and pEGFP-only treatment was monitored for 48 h. SCLN/siRNA complexes were added to the cells 24 h after administering SCLN/pEGFP. After 48 h, the cells were washed three times with cold PBS and fluorescent images of the cells were obtained using a Confocal Laser Scanning Microscope (Carl Zeiss, Germany).

2.8. In vivo toxicity of SCLN/DNA complexes

To identify the toxicity of the SCLN/DNA complexes, histological analysis was performed. Mice (BALB/C, female, 6 weeks old) were divided into three treatment groups of PBS (control), SCLN/pEGFP complexes, and SCLN/pEGFP/siRNA complexes (Table 1). Each sample was injected intravenously into the mice through the tail vein. Two days after injection, the mice were sacrificed. Their livers were removed and immediately fixed in 10% buffered formalin and embedded in paraffin. Sections were prepared for hematoxylin and eosin (H and E) stains.

2.9. In vivo gene delivery

Mice (BALB/C, female, 6 weeks old) were divided into four treatment groups that received either pEGFP vector alone, SCLN/pEGFP complexes, SCLN/pEGFP/siRNA complexes, or SCLN/siRNA complexes treated 24 h after an initial injection of SCLN/pEGFP complexes (Table 1). Each sample was injected intravenously into the mice through the tail vein. Two days after injection, the mice were sacrificed and their livers were removed. After washing with ice-cold PBS, the livers were frozen and cut into 6 μm thick cryosections. Fluorescence microscopy (Axiovision plus, Zeiss, Germany) was used to analyze pEGFP expression. To verify the existence of the SCLN/DNA complexes in the hepatocytes of the liver, transmission electron microscopy (TEM) was also performed.

3. Results

3.1. Characterization of SCLNs

WCS-LA conjugates were synthesized by forming an amide linkage between the carboxy group of LA and the amino group of WSC with EDC (Fig. 1). The conjugation of WSC and LA was confirmed by ^{1}H NMR analysis. The degree of substitution (DS) was calculated by comparing the ratio of methyl protons of LA to sugar protons, which for WSC was 43.7–100, respectively. Fig. 2 shows the results of the

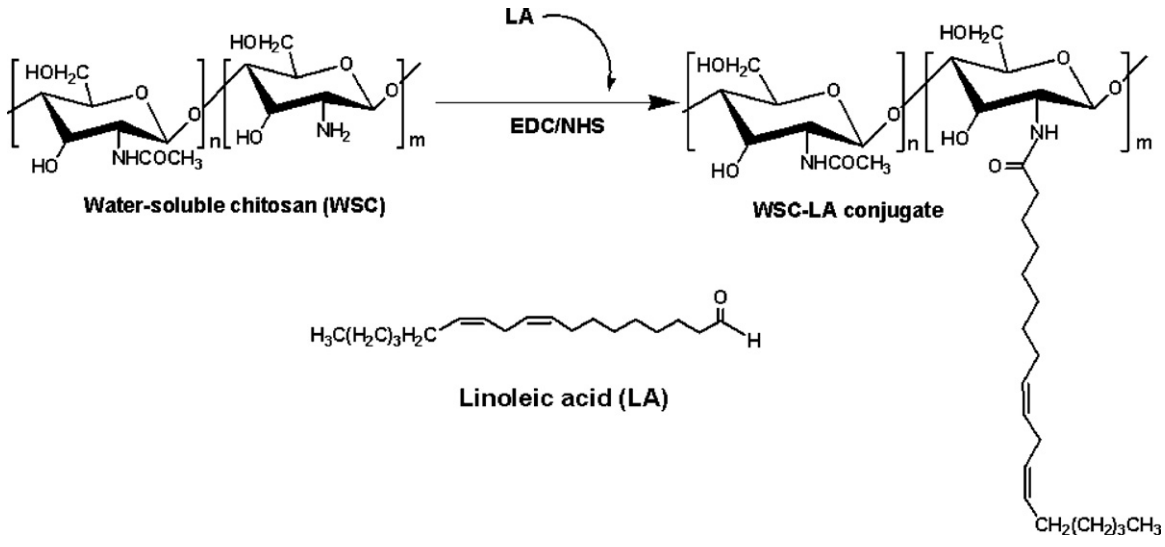

Fig. 1. Schematic illustration of the synthesis of the WSC-LA conjugates.

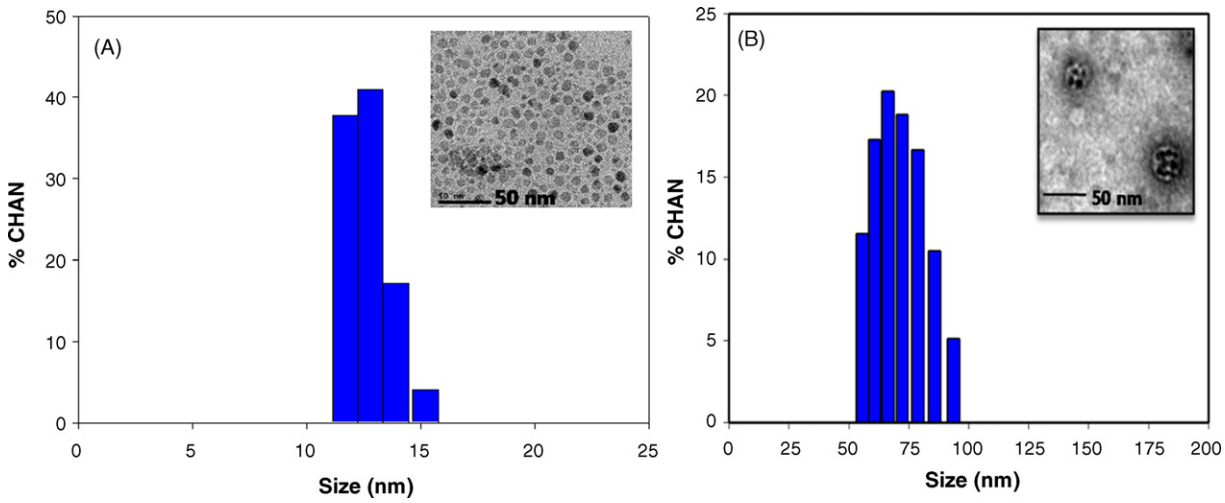

Fig. 2. Size distribution of SPIOs (A) and SCLNs (B) as measured by DLS. The inset shows a TEM image of SPIOs (A) and SCLNs (B), respectively.

size distribution and TEM images of SPION and SCLNs preparations. TEM images of the synthesized SPIONs showed that the nanoparticles were mostly spherical and uniform with a narrow distribution range (Fig. 2A). The mean size of the SPION particles was 11.7 nm as determined by dynamic light scattering (DLS). Oleic acid-coated SPIONs were loaded into self-assembled WSC-LA nanoparticles by a sonication and solvent-evaporation method. Clustering of SPIONs loaded into single WSC-LA nanoparticles was observed by TEM analysis after negative staining with phosphotungstic acid (PTA) (Fig. 2B). The mean size of SCLNs was approximately 67 ± 13 nm. To investigate the SPION loading in WSC-LA nanoparticles, TGA analysis was performed. TGA result revealed that the SPIONs account for approximately 37.68% (w/w) of the SCLNs.

3.2. Specific cellular uptake of SCLNs

In this study, we expected that SCLNs conjugated with LA would be specifically targeted to hepatocytes by lipid uptake in the liver. To investigate specific uptake, primary hepatocytes were isolated from mice and the cells were treated with various concentrations of ^{99m}Tc-labeled SCLNs. The radiolabeling efficiency was more than 97% and was stable for 6 h. As shown in Fig. 3, the count value of ^{99m}Tc taken up to the cells correlated well with the amount of SCLNs delivered. In the competition study, cellular uptake was significantly decreased by the addition of non-radiolabeled SCLNs.

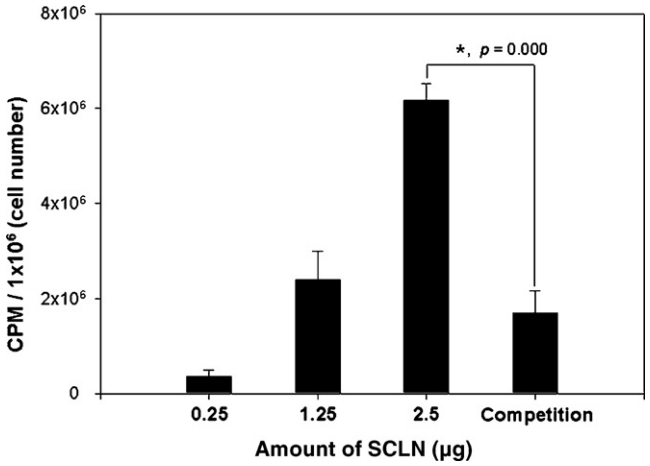

Fig. 3. Uptake of ^{99m}Tc-labeled SCLNs in hepatocytes. Each experiment was performed in triplicate. Values are expressed as a mean ± S.D. ($^{*}p < 0.0001$).

3.3. Nuclear and MR imaging

To examine the hepatocyte targeting ability of SCLNs, nuclear and MR imaging was performed using normal mice. Static images of ^{99m}Tc-labeled SCLNs in a mouse are shown in Fig. 4A. ^{99m}Tc-labeled SCLNs accumulated mainly in the liver within a few minutes after intravenous injection. T_2-weighted MR images of the middle part of the liver are shown in Fig. 4B. In addition, the signal intensity of the liver before and after injection of the SCLNs was slightly hyperintense compared to the back muscle before injection of SCLNs, while after injection of SCLNs, the signal of the liver became significantly darker than the back muscle. The reduction of T_2 signal in the liver was approximately 51.2%.

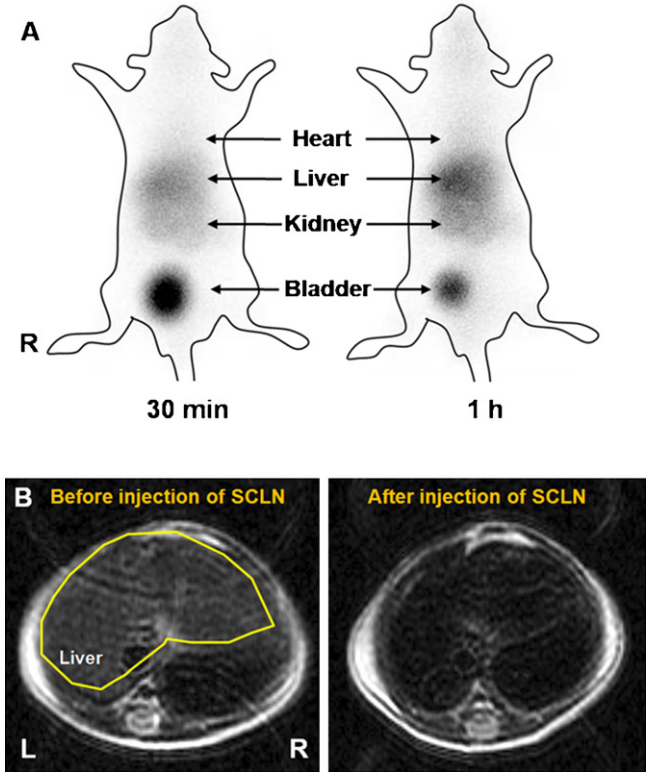

Fig. 4. Nuclear images (A) of mice at 30 min and 1 h after injection of ^{99m}Tc-labeled SCLNs. MR images (B) of the middle part of the mouse liver before and after injection of SCLNs.

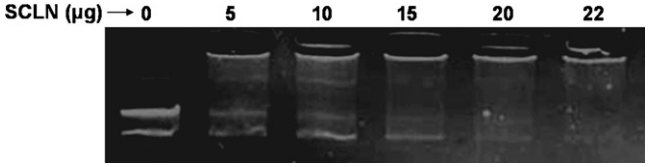

Fig. 5. Agarose gel electrophoresis retardation assay for SCLN/pEGFP/siRNA gene complexes.

3.4. Complex formation

Complete condensation of SCLNs and pEGFP was verified by agarose gel electrophoresis. Fig. 5 shows the photograph of the electrophoresis result for the SCLN/DNA complexes, which were formed by electrostatic interactions. Migration of the DNA on the gel decreased as the amount of SCLNs increased due to charge neutralization and increased molecular size of the complexes. Complete formation of the complexes occurred after addition of 22 μg of SCLNs. The size and zeta potential of the SCLN/DNA complexes was 95.3 nm and 49.8 mV, respectively (Table 1).

3.5. In vitro cell transfection

Expression of GFP and suppression by siRNA in hepatocytes using the SCLNs complexes were estimated by laser scanning confocal microscopy, as shown in Fig. 6. When naked pEGFP was incubated with hepatocytes, fluorescence was not detected (Fig. 6A and B). In contrast, GFP expression after treatment with the SCLN/pEGFP complexes was observed in the cytoplasm of hepatocytes (Fig. 6C and D). In addition, complexes containing siRNA suppressed the expression of GFP (Fig. 6E and F). Further, when SCLN/siRNA complexes were added to the media 24 h after the incubation with SCLN/pEGFP complexes was initiated, the expression of GFP was also down-regulated (Fig. 6G and H).

3.6. In vivo toxicity of SCLN/DNA complexes

To investigate the toxicity of SCLN/DNA complexes *in vivo*, hematoxylin and eosin staining of the livers was performed. There were no pathological changes in all groups. Comparing with the liver of the control mouse, histological characteristics of the livers of the mice treated with SCLN/pEGFP and SCLN/pEGFP/siRNA complexes were much similar without toxicity (Fig. 7A–C).

3.7. In vivo gene delivery

To investigate the potential of the new complexes to deliver specific genes *in vivo*, the SCLN/pEGFP complexes were injected through the tail vein of mice and the expression of the GFP gene in liver tissues was observed. Fig. 8 shows several fluorescence microscopic photographs taken of the expression of the GFP protein in the liver. When naked pEGFP was injected into mice, expression of GFP was rarely observed in the liver tissue (Fig. 8A). In contrast, treatment with the SCLN/pEGFP complexes resulted in high expression of the GFP gene product in the liver tissue, specifically in the cytoplasm of hepatocytes (Fig. 8B). Additionally, the expression of GFP introduced into hepatocytes by SCLN/pEGFP complexes was down-regulated *in vivo* by injecting complexes containing siRNA (Fig. 8C and D). To verify the presence of the SCLN/DNA complexes, the liver tissues were examined using a bio-TEM. As shown in Fig. 9, localization of iron nanoparticles was observed in hepatocytes. The particles had a well-formed spherical shape and compact structure. In particular, they were localized mainly in the mitochondria of hepatocytes.

4. Discussion

We describe a novel gene delivery imaging system based on self-assembled polymeric magnetic nanoparticles for targeting hepatocytes in this study. Our results indicate that polymeric magnetic nanoparticles, or SCLNs, are useful for both targeted gene transfer into hepatocytes as well as for hepatocyte-targeted MR imaging to monitor gene migration.

LA is one of the essential fatty acids and has a site for conjugation with hydrophilic polymers to give it amphiphilic properties, thereby creating the potential for self-assembly. Interestingly, when LA is injected into mice, it is largely taken up and metabolized in hepatocytes of liver. In addition, chitosan is a representative polymer for gene delivery. Thus, for our study, we made use of

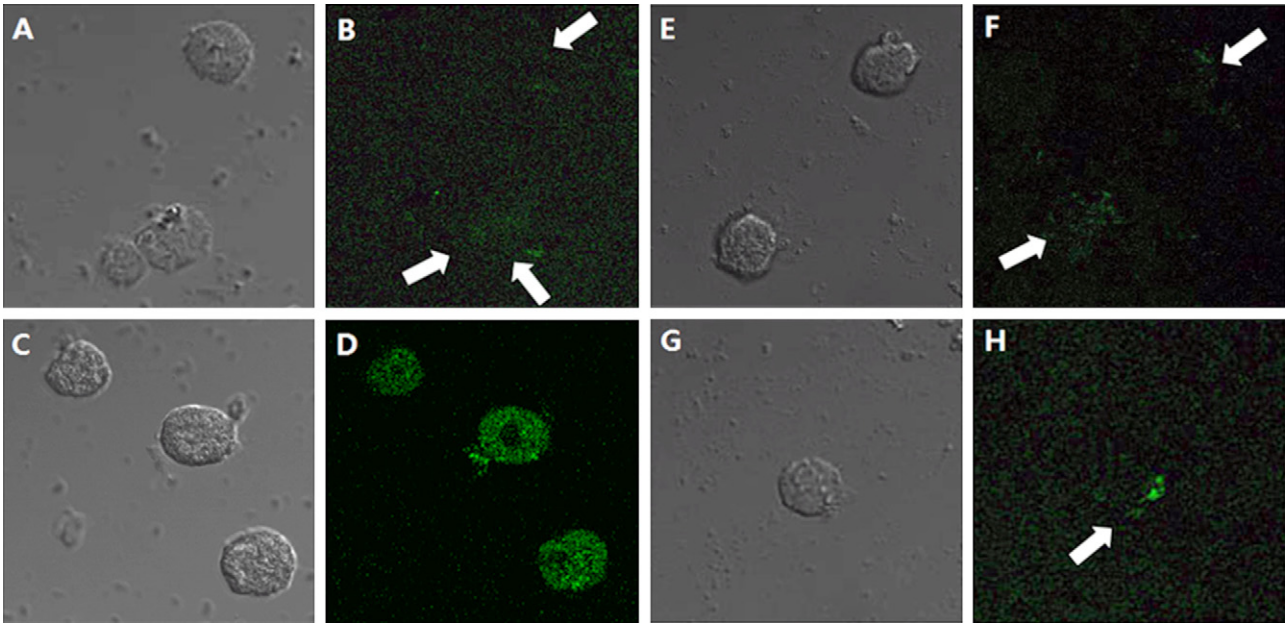

Fig. 6. Confocal micrographs in primary hepatocytes 48 h after incubation with pEGFP only (A and B), SCLN/pEGFP complexes (C and D), SCLN/pEGFP/siRNA complexes (E and F), and SCLN/siRNA complexes (G and H), the latter of which was added to cell culture media 24 h after treatment of hepatocytes with SCLN/pEGFP complexes.

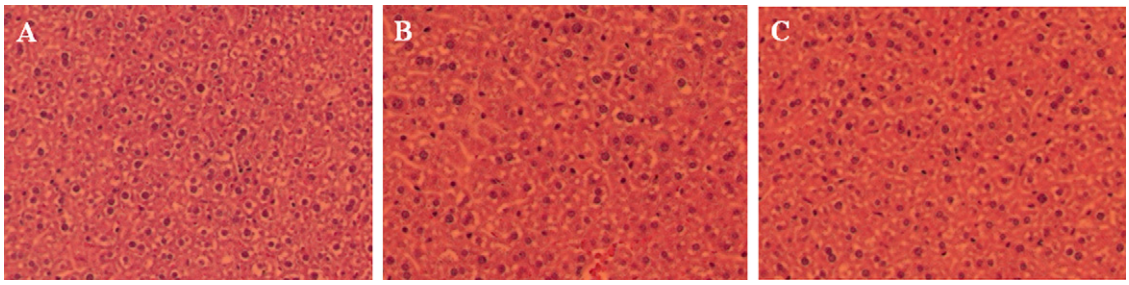

Fig. 7. Histological examination of liver tissue. Hematoxylin and eosin stained sections of liver from a PBS injected mouse (A), SCLN/pEGFP complexes injected mouse (B) and SCLN/pEGFP/siRNA complexes injected mouse (C).

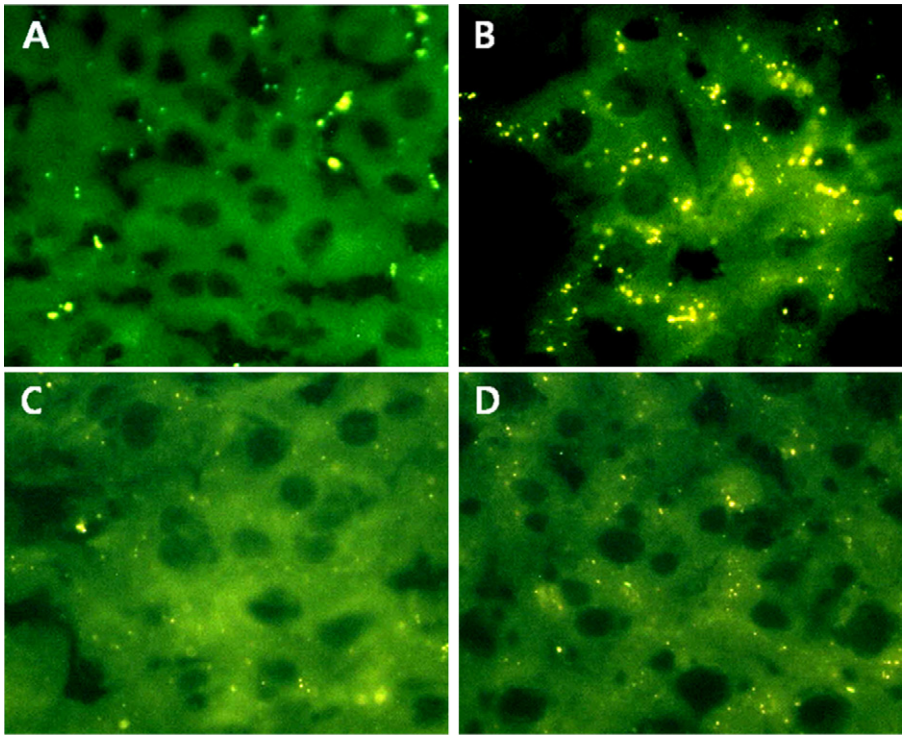

Fig. 8. Fluorescence micrographs of mouse livers 48 h after intravenous injection of pEGFP (A), SCLN/pEGFP complexes (B), SCLN/pEGFP/siRNA complexes (C), and SCLN/siRNA complexes (D). The agents were injected into the tail vein 24 h after the SCLN/pEGFP complexes were initially administered.

the following properties of WSC, LA, and SPIONs: (1) amphiphilic polymers based on WSC and LA readily self-assemble in aqueous solution; (2) LA in the core of self-assembled nanoparticles can provide an entrapment force for oleic acid-coated SPIONs; (3) WSC in the shell part of the nanoparticles can form electrostatic complexes with DNA; and (4) by introducing LA, SCLNs, and SCLN/DNA, complexes based on WSC-LA conjugates can be taken up by hepatocytes specifically (Scheme 1).

WSC-LA conjugates readily self-assembled in aqueous solution into core–shell structures with a diameter of 50–100 nm. The hydrophobic core of the WSC-LA nanoparticles allows for incorporation of hydrophobic drugs and oleic acid-coated SPIONs. Indeed,

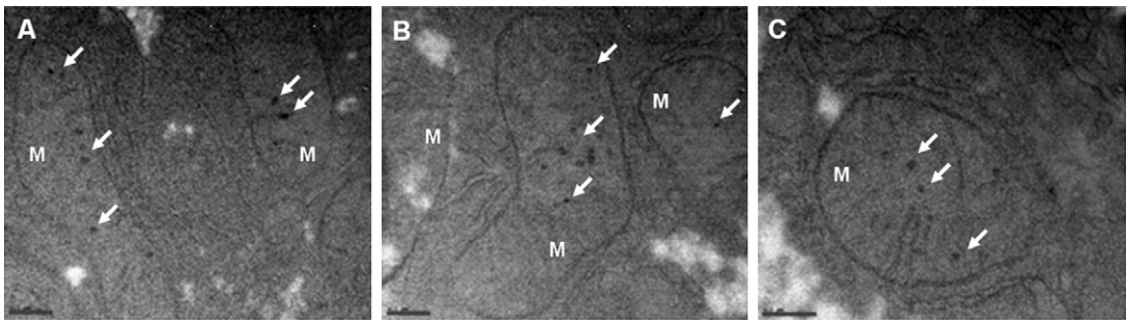

Fig. 9. BioTEM images of hepatocytes in the liver selected from mice after injection of SCLN/pEGFP complexes (A), SCLN/pEGFP/siRNA complexes (B), and SCLN/siRNA complexes (C), which was injected into the tail vein 24 h after the SCLN/pEGFP complexes were initially administered. SCLNs were localized mainly in the cytoplasm of hepatocytes, especially in the mitochondria. White arrows indicate SCLNs scattered in the mitochondria of hepatocytes. The scale bar is 100 nm. "M" denotes mitochondria.

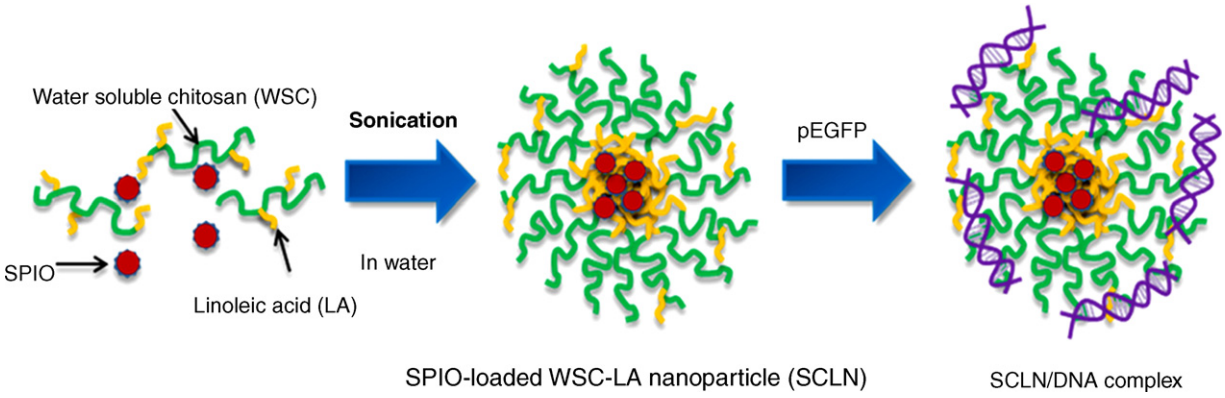

Scheme 1. Schematic illustration of the formation of SCLN and SCLN/DNA complexes.

SPIONs were incorporated into the WSC-LA nanoparticles, and formed a cluster in the core (Fig. 2). These SPION clusters exhibit a high magnetic responsiveness in MR imaging (Reimer et al., 2000).

SCLNs were specifically driven to the hepatocytes by LA, which accumulates in hepatocytes and plays a central role in the liver. Internalization into hepatocytes was investigated by cellular uptake of radiolabeled SCLNs (Fig. 3). Further, treatment with non-radiolabeled SCLNs decreased the cellular uptake of radiolabeled SCLNs in hepatocytes. Previous reports have used essential polyunsaturated fatty acids to demonstrate that the liver plays a central role in providing fatty acids during hepatic diseases and cholestatic diseases (Picard et al., 1972; Owen et al., 1982). In particular, Thomas et al. (1988) reported that linoleic acid moves into hepatocytes through selective channeling of arachidonic and linoleic acids into glycerolipids of rat hepatocytes. Taken together, these findings suggest that the SCLNs used in this study accumulated specifically in liver hepatocytes.

Molecular imaging is a novel tool that has allowed non-invasive diagnostic imaging to advance beyond gross anatomical description to identification of specific tissues and observation of biological processes at the cellular level (Weissleder, 1999). Recent advances in nanotechnology have extended this research to include MR imaging. Indeed, the exploitation of nanotechnology for MR molecular imaging has generated several candidate contrast agents. As a multimodality platform, SPIONs are useful for non-invasive detection (Thorek et al., 2006). Further, SPIONs with modified surface coats can be used for receptor-directed imaging, cell labeling for *in vivo* monitoring of cell migration, e.g., stem cell labeling, and labeling of gene constructs for localization in gene therapy. If gene complexes can form using SPIONs, the accumulation of the gene *in vivo* can be observed non-invasively through MR imaging. In this study, nuclear and MR imaging showed that SCLNs accumulated in the liver (Fig. 4). Therefore, we hypothesized that if SCLNs could be complexed with a gene, SCLNs could also be used as imaging probes for tracking the movement of the gene.

Formation of the SCLN/pEGFP complexes was analyzed using a gel retardation assay (Fig. 5). Complete condensation between SCLNs and pEGFP was achieved by electrostatic binding between the cationic polyelectrolyte chitosan and the negatively charged DNA. Chitosan has been used for gene delivery previously due to its cationic properties, bioavailability, and low toxicity, and gene carriers composed of chitosan show high transfection efficiency and can be used successfully as non-viral gene delivery system both *in vitro* and *in vivo* (Borchard, 2001; Mansouri et al., 2004; Gao et al., 2005; Richardson et al., 1999).

When the SCLN/pEGFP complexes were transfected into primary hepatocytes, GFP expression was seen in the cytoplasm. In addition, when complexes containing siRNA were transfected into cells, suppression of GFP expression was observed (Fig. 6). We interpreted these results to mean that SCLNs were able to successfully deliver a gene and siRNA into hepatocytes.

Next, to investigate the specific gene delivery capacity of SCLNs *in vivo*, SCLN/pEGFP complexes were injected into mice and GFP expression in liver tissues was analyzed. As expected from our *in vitro* study, GFP expression was detected specifically in the cytoplasm of hepatocytes, while GFP expression was suppression by the addition of siRNA complexes (Fig. 8).

Therapy using gene silencing by siRNA may be effective for the treatment of various viral diseases, such as hepatitis B or C viruses. Based on our results, we conclude that SCLNs might be useful for such siRNA-based therapeutic applications. Finally, to verify that SPIONs were actually present in hepatocytes, liver tissues were observed using a bio-TEM, which indicated that iron nanoparticles were indeed localized into hepatocytes (Fig. 9). Hepatocyte-selective accumulation of the SCLN/pEGFP complexes was also confirmed by TEM analysis.

In conclusion, we have developed a novel gene delivery imaging system that allows for hepatocyte-selective imaging and gene delivery. Targeted delivery of plasmid DNA into hepatocytes was successfully carried out both *in vitro* and *in vivo* using SCLNs. The SCLN complexes containing siRNA suppressed GFP expression in hepatocytes. Furthermore, the selective accumulation of SCLN/gene complexes in hepatocytes could be monitored by MR imaging. Therefore, we believe that SCLNs are a very useful platform for gene delivery and for tracking gene mobility. We are especially interested in the possibility of targeting SPION particles to mitochondria, as was observed in this study; this will be the focus of future investigations.

Acknowledgments

This study was supported by grants from the National R&D Program for Cancer Control, Ministry for Health, Welfare and Family affairs, Republic of Korea (0620220 and 0720420). This work was also supported by Nuclear R&D program through the Korea Science and Engineering Foundation funded by the Ministry of Science & Technology (M20702000003-08N0200-00310).

References

Adrian, J.E., Poelstra, K., Scherphof, G.L., Meijer, D.K., van Loenen-Weemaes, A.M., Reker-Smit, C., Morselt, H.W., Zwiers, P., Kamps, J.A., 2007. Effects of a new bioactive lipid-based drug carrier on cultured hepatic stellate cells and liver fibrosis in bile duct-ligated rats. J. Pharmacol. Exp. Ther. 321, 536–543.
Borchard, G., 2001. Chitosan for gene delivery. Adv. Drug Deliv. Rev. 52, 145–150.
Bulte, J.W., Kraitchman, D.L., 2004. Iron oxide MR contrast agents for molecular and cellular imaging. NMR Biomed. 17, 484–499.

Davis, M.E., 2002. Non-viral gene delivery systems. Curr. Opin. Biotechnol. 13, 128–131.
Erbacher, P., Zou, S., Bettinger, T., Steffan, A.M., Remy, J.S., 1998. Chitosan-based vector/DNA complexes for gene delivery: biophysical characteristics and transfection ability. Pharm. Res. 15, 1332–1339.
Gao, S., Chen, J., Dong, L., Ding, Z., Yang, Y.H., Zhang, J., 2005. Targeting delivery of oligonucleotide and plasmid DNA to hepatocyte via galactosylated chitosan vector. Eur. J. Pharm. Biopharm. 60, 327–334.
Jun, Y.W., Huh, Y.M., Choi, J.S., Lee, J.H., Song, H.T., Kim, S., Yoon, S., Kim, K.S., Shin, J.S., Suh, J.S., Cheon, J., 2005. Nanoscale size effect of magnetic nanocrystals and their utilization for cancer diagnosis via magnetic resonance imaging. J. Am. Chem. Soc. 127, 5732–5733.
Kim, E.M., Jeong, H.J., Kim, S.L., Sohn, M.H., Nah, J.W., Bom, H.S., Park, I.K., Cho, C.S., 2006. Asialoglycoprotein-receptor-targeted hepatocyte imaging using ^{99m}Tc galactosylated chitosan. Nucl. Med. Biol. 33, 529–534.
Liu, C.G., Desai, K.G., Chen, X.G., Park, H.J., 2005. Linoleic acid-modified chitosan for formation of self-assembled nanoparticles. J. Agric. Food Chem. 53, 437–441.
Mansouri, S., Lavigne, P., Corsi, K., Benderdour, M., Beaumont, E., Fernandes, J.C., 2004. Chitosan-DNA nanoparticles as non-viral vectors in gene therapy: strategies to improve transfection efficacy. Eur. J. Pharm. Biopharm. 57, 1–8.
Nishikawa, M., Takemura, S., Takakura, Y., Hashida, M., 1998. Targeted delivery of plasmid DNA to hepatocytes in vivo: optimization of the pharmacokinetics of plasmid DNA/galactosylated poly(L-lysine) complexes by controlling their physicochemical properties. J. Pharmacol. Exp. Ther. 287, 408–415.
Owen, J.S., Bruckdorfer, K.R., Day, R.C., McIntyre, N., 1982. Decreased erythrocyte membrane fluidity and altered lipid composition in human liver disease. J. Lipid Res. 23, 124–132.
Pandey, N.R., Renwick, J., Misquith, A., Sokoll, K., Sparks, D.L., 2008. LA-enriched phospholipids act through peroxisome proliferator-activated receptors to stimulate hepatic apolipoprotein A-I secretion. Biochemistry 47, 1579–1587.
Picard, J., Veissiere, D., Voyer, F., 1972. Identification of the apolipoprotein of abnormal serum lipoproteins in cholestasis. Clin. Chim. Acta 37, 483–489.
Ponder, K.P., 1996. Analysis of liver development, regeneration, and carcinogenesis by genetic marking studies. FASEB J. 10, 673–682.
Reimer, P., Jähnke, N., Fiebich, M., Schima, W., Deckers, F., Marx, C., 2000. Hepatic lesion detection and characterization: value of nonenhanced MR imaging, superparamagnetic iron oxide-enhanced MR imaging, and spiral CT-ROC analysis. Radiology 217, 152–158.
Richardson, S.C., Kolbe, H.V., Duncan, R., 1999. Potential of low molecular mass chitosan as a DNA delivery system: biocompatibility, body distribution and ability to complex and protect DNA. Int. J. Pharm. 178, 231–243.
Sagara, K., Kim, S.W., 2002. A new synthesis of galactose-poly(ethylene glycol) polyethylenimine for gene delivery to hepatocytes. J. Control. Release 79, 271–281.
Seglen, P.O., 1976. Preparation of isolated rat liver cells. Methods Cell Biol. 13, 29–83.
Sun, S., Zeng, H., Robinson, D.B., Raoux, S., Rice, P.M., Wang, S.X., Li, G., 2004. Monodisperse MFe_2O_4 (M = Fe, Co, Mn) nanoparticles. J. Am. Chem. Soc. 126, 273–279.
Thomas, G., Loriette, C., Pepin, D., Chambaz, J., Bereziat, G., 1988. Selective channelling of arachidonic and linoleic acids into glycerolipids of rat hepatocytes in primary culture. Biochem. J. 256, 641–647.
Thorek, D.L., Chen, A.K., Czupryna, J., Tsourkas, A., 2006. Superparamagnetic iron oxide nanoparticle probes for molecular imaging. Ann. Biomed. Eng. 34, 23–38.
Walther, W., Stein, U., 2000. Viral vectors for gene transfer: a review of their use in the treatment of human diseases. Drugs 60, 249–271.
Weissleder, R., 1999. Molecular imaging: exploring the next frontier. Radiology 212, 609–614.
Weissleder, R., Mahmood, U., 2001. Molecular imaging. Radiology 219, 316–333.
Wu, J., Nantz, M.H., Zern, M.A., 2002. Targeting hepatocytes for drug and gene delivery: emerging novel approaches and applications. Front. Biosci. 7, 717–725.